Biointerface Research in Applied Chemistry
Open-Access Journal (ISSN: 2069-5837)

Article
Volume 13, Issue 5, 2023, 416
https://doi.org/10.33263/BRIAC135.416

Evaluation of Microhardness, Wear, and Corrosion Behavior of Duplex Ni-P/Ni-W-P Coatings

Palash Biswas [1], Suman Kalyan Das [1], Prasanta Sahoo [1,*]

[1] Department of Mechanical Engineering, Jadavpur University, Kolkata 700032, India
* Correspondence: psjume@gmail.com; prasanta.sahoo@jadavpuruniversity.in (P.S);

Scopus Author ID 55562055400
Received: 25.07.2022; Accepted: 30.08.2022; Published: 22.11.2022

Abstract: Electroless Ni-P/Ni-W-P coatings in the duplex form are deposited on mild steel substrates. These deposits were subjected to heat treatment with different temperatures (200 to 800°C) and for time periods of 1h & 4h. Heat treatment condition has a significant influence on the coating properties. The coatings' microhardness and wear resistance increase significantly when heat is treated up to 400°C temperature. However, there is a degeneration in the microhardness when the coatings are treated beyond 400°C and also for 4h duration. This is due to coarsening of grains together with the formation of oxides, as indicated by the microstructural studies. At a heat treatment temperature of 800°C for 4h, the coating exhibits cracks and tends to delaminate. The wear mechanism encountered during the sliding test under dry conditions and at room temperature is predominantly abrasive. The electrochemical-based corrosion studies indicate that corrosion resistance of the present duplex coatings increases after heat treatment which may be due to the coarsening of grains. Finally, the comparison is made between the performances of the present duplex coatings to the constituent binary coatings. Overall, it is found that upon being subjected to the optimal condition of heat treatment, the duplex coating presents an all-around performance that may be suitable for applications demanding both wear and corrosion resistance. This will lead to their application in bio-tribology-related applications.

Keywords: electroless; deposit; microstructure; heat treatment; friction; tribology.

1. Introduction

The electroless Nickel (EN) deposition procedure is widely practiced, providing several advantages over conventional coating techniques relevant to industries. Brenner and Riddell invented this method of deposition in 1946 [1]. The deposition process eliminates the need for electricity as it is an autocatalytic reduction process. EN coating has obtained popularity because of its uniformity, higher hardness, lower wear rate, and better corrosion resistance. EN coating is now considered an effective surface engineering technique for changing the physicochemical properties of the substrate surface. The coating can be homogeneously deposited on any irregular shape, surface, or geometry. Due to these aspects, Ni-P coatings are suitable for all industries, from food processing to aerospace [2]. Moreover, due to its deposition uniformity and moderate bio-compatibility, EN coatings have been applied to medical devices for protection against corrosion. Some medical components on which EN coatings have been applied include anesthesia delivery components, laryngoscope handles, radiation focus plates, radiation lead, etc. [3].

Ni-P coating is a supersaturated compound. Upon heat treatment at appropriate conditions, nickel phosphide phases form, which precipitate at the grain boundaries, inhibiting the movement of dislocations. This enhances the strength and hardness of the coating. Alternatively, when a third element is introduced in the Ni-P matrix, it provides additional advantages to the Transition metal, viz. Tungsten (W), when incorporated in Ni-P coatings, improves its mechanical properties and results in higher wear resistance [4-6]. Since the melting point of W is relatively higher, its incorporation further leads to the excellent thermal stability of the coating [7]. Recently duplex, multilayer, and graded coatings have been developed, keeping in mind the multifunctional applications demanded in many industries. Duplex or multilayer coatings acquire the constituent coatings' best properties and are expected to have enhanced mechanical and tribological properties. The electroless process may develop the duplex/multilayer coatings by sequential immersion of the substrate in desired baths for a predefined period. Multilayer Ni-P/Ni-B have been developed to study their friction and wear behavior [8]. Duplex Ni-P/Ni-W-P coating has been successfully deposited on magnesium alloy with a smooth appearance. After laser treatment, the microhardness of the coating increases [9]. Graded Ni-P coatings have been successfully realized with variation in P content across the layers, and their corrosion and wear behavior has been reported [10].

The current work develops duplex Ni-P/Ni-W-P coatings through an electroless technique. Ni-W-P being harder is expected to provide resistance against wear and hence is positioned as the external layer. At the same time, Ni-P provides the necessary corrosion resistance and serves as the inner layer. Ni-P coating gets its corrosion resistance mainly due to the development of the passive film. This film is responsible for resisting attack by the corrosive media. The coatings are heat treated at different temperatures and durations. Characterization of the coatings is carried out with the aid of a Scanning Electron Microscope (SEM) (detailed microscopy), Energy dispersive X-ray analysis (EDX) (for detecting the constituents), and X-ray diffraction analysis (XRD) (for detecting the phases). The tribological testing of coated samples is carried out on a pin-on-disc setup. A microhardness test is carried out to evaluate the mechanical properties of the coated samples. Corrosion tests are conducted by potentiodynamic polarization (PDP) and electrochemical impedance spectroscopy (EIS) techniques.

2. Materials and Methods

2.1. Coating deposition.

Mild steel substrates are chosen for the deposition. As EN coating follows the substrate surface profile, substrates with similar roughness values are chosen for deposition. Prior to deposition, samples are cleaned of rust and other foreign materials using acetone and HCl solution. For deposition of the inner layer, the substrate is first dipped in the Ni-P bath [11] for 2 hours and then in the Ni-W-P bath [12] for another 2 hours. For the coating deposition, the source of Ni (Nickel) and tungsten are Nickel-sulfate ($NiSO_4(H2O)_6$) and Sodium tungstate (Na_2WO_4), respectively. Sodium hypophosphite ($NaPO_2H_2$) acts as the reducing agent. The dual bath technique is used to deposit two successive layers of Ni-P (inner) and Ni-W-P (outer) over the mild steel substrates [13]. Heat treatment of the coating is carried out at temperatures ranging from 200°C to 800°C with time durations of 1 and 4h in a Muffle Furnace by Electro Scientific Equipment, Howrah (India) (Model No. ESE, Temperature range: RT-1450°C) with no special environment. The rate of heating is kept fixed at 10°C per minute. Phase

transformation of EN coatings occurs above a certain heat treatment temperature [14]. After the heat treatment process is over, the samples are extracted and air-cooled.

2.2. Microhardness measurement.

The micro-hardness of the samples was analyzed by Walter UHL Technische Mikroskopie (VMHT-MOT). The test is conducted by employing the following test parameters: load 100 g-f, speed 25 μm/s, and dwell time 15s. The mean microhardness value has been reported in the current study. The indentation depth is measured by an optical microscope.

2.3. Microstructural study of coating.

As part of a microstructural study of the coatings, the surface morphology is observed with the help of a Field Emission Scanning Electron Microscope (FESEM) by Carl Zeiss, Germany (Model No. EVO LS 10). Everhart-Thornley Detector is used to detect the secondary electrons (SE). EDX is used to determine phosphorus, tungsten, nickel, and chromium content in the coatings.

XRD by Rigaku, Japan (Ultima III) is used for analyzing the phase structure of the coating. Based on the literature survey, a diffraction angle (2θ) range between 20-80° is selected [15]. The scanning speed is fixed at 1.0°/min. The sharp peak in the plot indicates the presence of a crystalline phase, while diffused peaks are indicative of an amorphous phase [16].

2.4. Tribological test.

Tribological tests are performed in the pin-on-disc arrangement. The corresponding setup used is by Ducom, India (TR-20LE-CHM-400) at ambient temperature and under dry conditions. All the tests are carried out as per ASTM G99. The counterface disc is made of hardened steel. A constant applied load of 20N at 50 RPM (for 60 mm track diameter) is selected based on previous work [17]. The total sliding distance was also kept constant (about 95m) for each sample. The friction was represented in terms of the coefficient of friction (cof) which was directly captured by the system. However, for determining the wear rate (K), the weight loss of the samples after each test is measured. And the wear volume is divided by the sliding distance as well as by the normal load.

2.5. Corrosion test.

Corrosion tests are evaluated in 3.5 wt. percent brine solution using a potentiostat/galvanostat by ACM Instruments, UK (Gill AC). The data for the Tafel curve and impedance charts are generated employing a three-electrode setup [18,19]. The scanning rate is fixed at 1mV/s during the PDP tests. The system's open circuit potential (OCP) takes 10 min to settle down. The starting and inverse potential are considered as -250mv and 250mv, respectively. The area in contact with the NaCl solution for all samples is kept constant at $1cm^2$.

3. Results and Discussion

3.1. Microstructure characterization.

The surface morphology of duplex electroless Ni-P/Ni-W-P coatings is investigated with the aid of SEM micrographs (Figure 1). As deposited coatings display nodular structure

with nodule size ranging between 5 -10 µm. With heat treatment, however, the size of the nodule changes (Figure 1b-f). This may also be indicative of changes in its microstructure. It is found that with heat treatment, the nodules undergo bulging (Figure 1b). The bulging is more prominent for prolonged heat treatment (Figure 1c). However, upon heat treatment at 600°C and beyond, the nodules seem to undergo flattening (Figure 1e). The sample heat treated at 800°C for 4h develops cracks (indicated by arrows) on the surface (Figure 1f) which is due to the relief of the accumulated thermal stress in the coating microstructure. Apart from these, some dark spots are noticed on the coating surface. For samples heat treated at 600°C and 800°C, these dark spots are more prominent. The presence of dark patches may indicate that oxides may have formed on the coating surface.

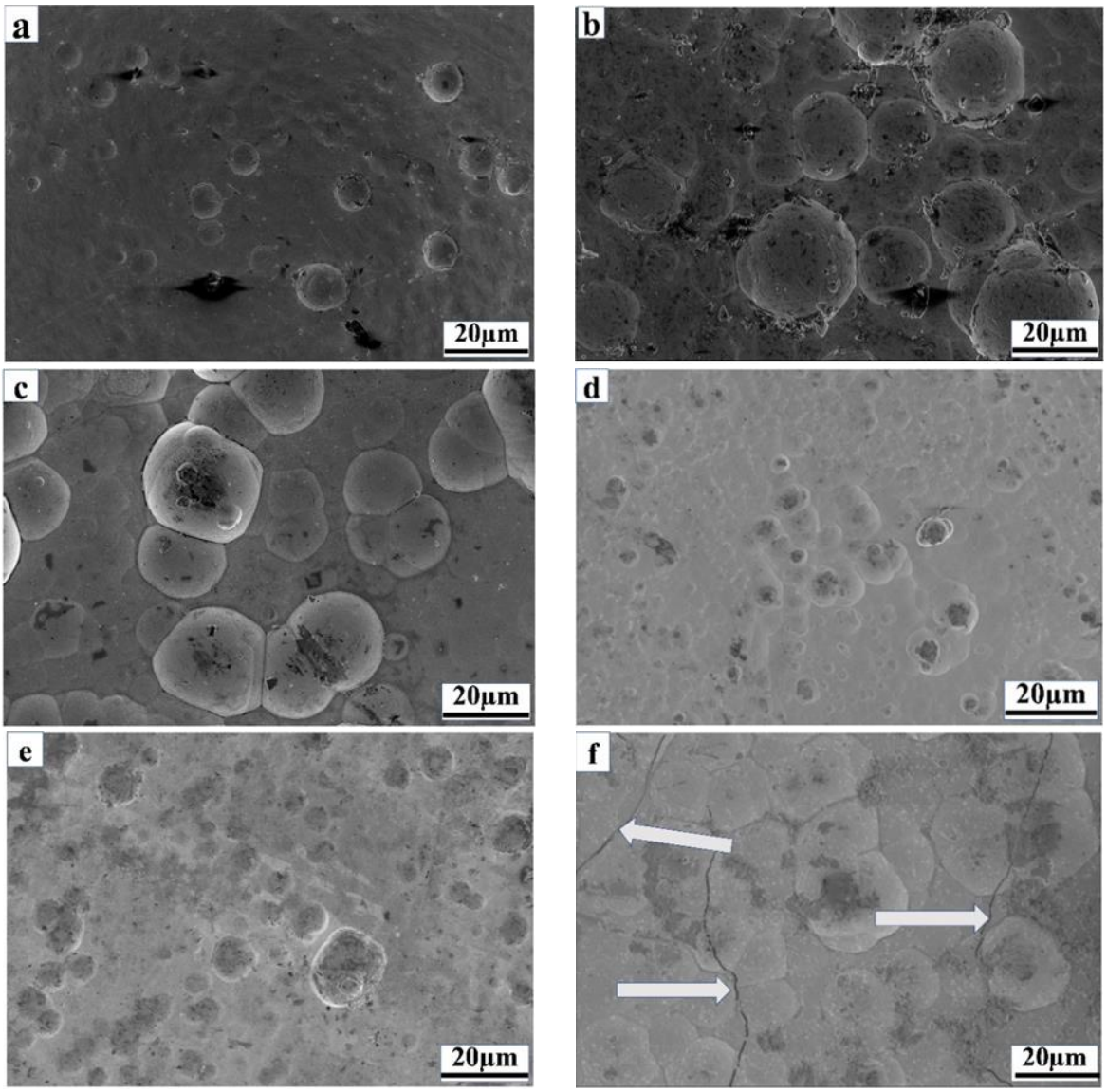

Figure 1. FESEM images of **(a)** as-deposited coating; **(b)** 400°C for 1h duration; **(c)** 400°C for 4h duration; **(d)** 600°C for 1h duration; **(e)** 800°C for 1h duration; **(f)** 800°C for 4h duration.

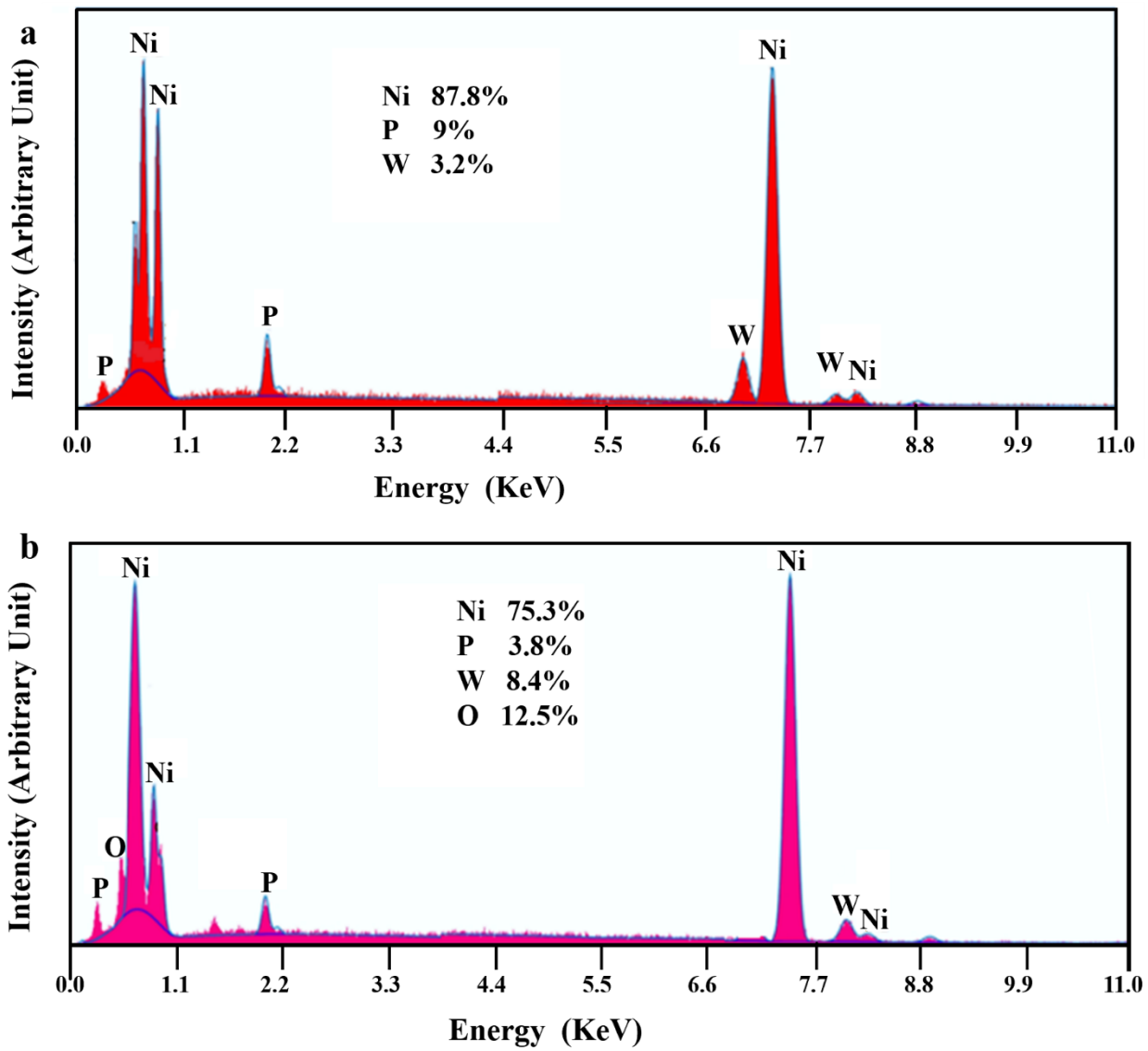

Figure 2. EDX line spectrum of **(a)** as-deposited coating; **(b)** heat treated at 800°C, 4h.

Table 1. EDX data of the as-deposited samples.

Duplex Ni-P/Ni-W-P Samples	Elements in wt.%			
	P	W	Ni	O
As-deposited	9.00	3.20	87.80	-
Heat treated at 400°C, 1h	7.80	4.10	88.10	-
Heat treated at 800°C, 4h	3.80	8.40	75.30	12.50

The EDX spectrum of Ni-P/Ni-W-P coating is presented in Figure 2, along with the constituents' percentage composition in Table 1. It is observed that the current electroless nickel coating has a moderately higher percentage of phosphorous. Hence, the deposit is expected to be amorphous/micro-crystalline [10]. Marginal variation in the concentration of the constituents is noticed for samples after heat treatment due to the changes in the coating microstructure. The samples heat treated beyond 400°C show oxygen as one of the constituents (Figure 2b), which confirms the occurrence of oxidation in the coating at higher temperature heat treatment. Additionally, the line EDX is performed on the cross-section of the coating, as shown in (Figure 3a), and the corresponding plot is presented in (Figure 3b). From the cross-cut micrograph, the overall thickness of the present coating is found to be around 40µm. But, there is no visible demarcation between the two layers of the coating. From line EDX results, it can however be seen that W is detected from the top surface of the coated sample up to about

a depth of 18µm. Beyond this zone, only Ni and P are detected at their usual concentration until about 40µm after which Fe becomes the dominant phase. This confirms the successful deposition of two layers of the coating as expected. The absence of visible demarcation in the cross-cut micrograph may indicate splendid adhesion and compatibility between the two layers of the deposit.

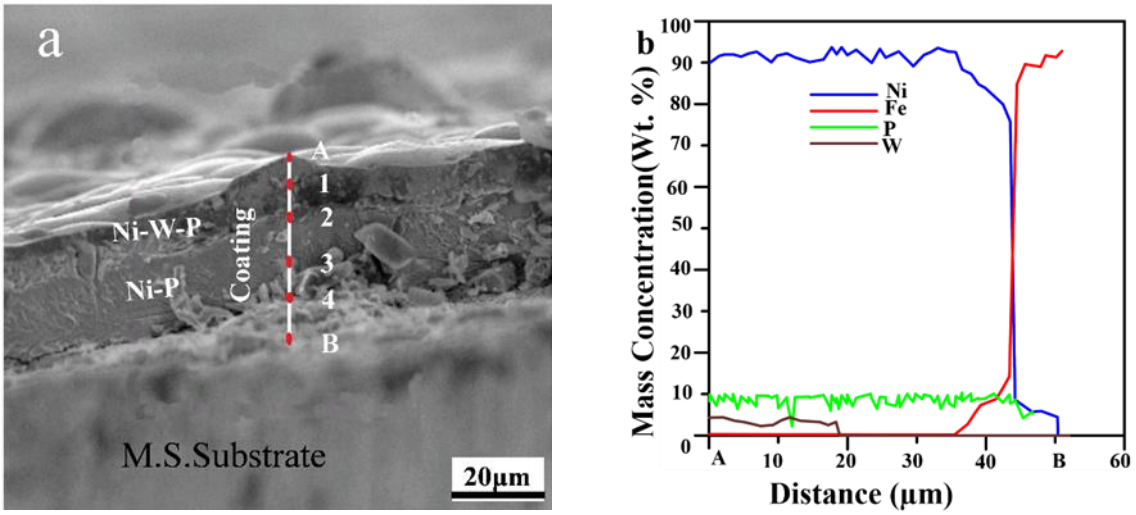

Figure 3. FESEM images of **(a)** coating cross-section showing line EDX of deposit; **(b)** composition profile of deposit.

3.2. Phase structure.

XRD analysis of coating is presented in Figure 4. The as-deposited sample exhibits mainly an amorphous structure typical to any high phosphorous electroless nickel deposit. This is represented by the XRD plot exhibiting a single broad peak ranging between 2θ values of 35-55°. Now, when heat is treated at 200°C, there is not much change in the XRD plots. However, when the samples are heat treated at/beyond 400°C, there is a marked change in the samples' XRD profile with multiple peaks of various phases combining Ni, P, W, and even O. This shows a phase transformation in the coating microstructure when heat treated at a temperature between 200 and 400°C. One of the previous literature dealing with similar coating reports the phase transformation occurring at a temperature of around 350°C [20]. One of the important phases detected in the present coating after heat treatment is the stable nickel phosphide (Ni_3P) phase, which is responsible for the coating's increase in hardness and wears resistance. In fact, for samples heat treated at 400°C, 1h, many nickel phosphide (Ni_3P) phases are detected in different planes like (301), (321), (330), and (141). As a transformation to Ni_3P occurs more at around 400°C temperature, these samples are expected to possess higher hardness and wear resistance than other treated samples. Apart from that Ni (111) phase is also detected. No metastable phases of nickel and phosphorous are detected. One of the interesting phases to be detected is the WP phase. With an increased duration of heat treatment at 400°C, the number of crystalline peaks is found to be somewhat reduced. When the heat treatment temperature increases or even for a higher treatment duration, the peaks in the XRD profiles get sharper, this sharpening of the peaks may occur as a result of relaxation in the surface strain and increased grain size growth [21].

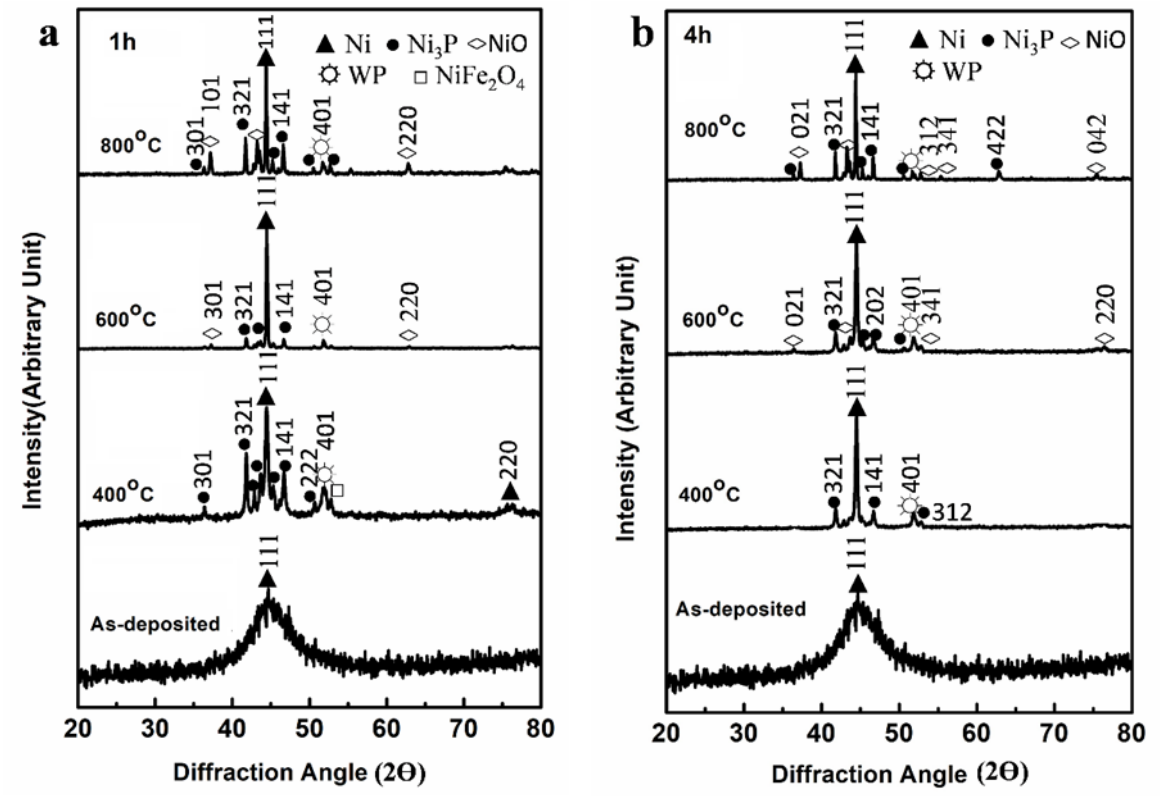

Figure 4. XRD plots for heat-treated samples **(a)** 1h duration; **(b)** 4h duration.

Heat treatment at 600°C and 800°C reveal oxide phases of nickel oxide (NiO), implying the formation of oxides, as also indicated in the EDX results previously. NiO being dark green in color, generate visible dark patches on the coating surface. A significant difference isn't observed in comparing the XRD plots of 1h and 4h heat treatment durations. However, the increased detection of the oxide phase at higher temperatures for 4h duration cycles may moderately influence the tribological and corrosion behavior of the present duplex coatings.

3.3. Microhardness study.

Electroless nickel coating is inherently hard. Further, in the case of duplex coatings, the combined microhardness of the individual layers, reported as the indenter, is expected to penetrate both layers (considering the thickness of the individual layers of deposits and the load applied). The microhardness of as-deposited duplex coatings in the present investigation is reported as 724 $HV_{0.1}$. In fact, for better visualization, the microhardness results for all the samples are presented in the form of plots, as shown in Figure 5a. Heat treatment seems to have a direct impact on the microhardness of the coating. The microhardness almost doubles that of as-deposited microhardness at a heat treatment cycle of 400°C and 1h. This shows the microhardness of the coating is most impacted post the phase transformation regime and the formation of various crystalline phases, particularly Ni_3P phase. Ni_3P phase being a hard phase, come in the way of dislocation resisting them. The dislocations, which are favorable for progressing in amorphous substance, get impeded by the grain boundaries in crystalline structures. These combined phenomena result in the samples being heat treated at 400°C and 1h to display the best microhardness. It is interesting to see that despite oxidation getting initiated at 600°C, 1h heat treatment cycle, the microhardness of the deposit doesn't suffer much (refer to Figure 5a). However, when heat treated at 800°C, 1h, the microhardness of the coated sample reduces drastically. This is mainly due to grain coarsening as well as oxide formation.

Upon heat treatment for 4h duration, the hardness is more than that of as-deposited hardness. But the values are significantly lesser than that observed for 1h heat-treated specimens. For a 4h sample, the formation of Ni_3P phases may be lesser, as indicated in XRD results. At the same time, for a 4h heat treatment cycle, there is a higher accumulation of thermal stresses, which act as residual stresses and hence result in a quicker formation and movement of dislocations. The best microhardness for 1h and 4h heat treatment cycles are compared to as-deposited microhardness and presented in (Figure 5b). It can be observed that w.r.t. microhardness, the 1h heat treatment duration seems to be the optimum choice.

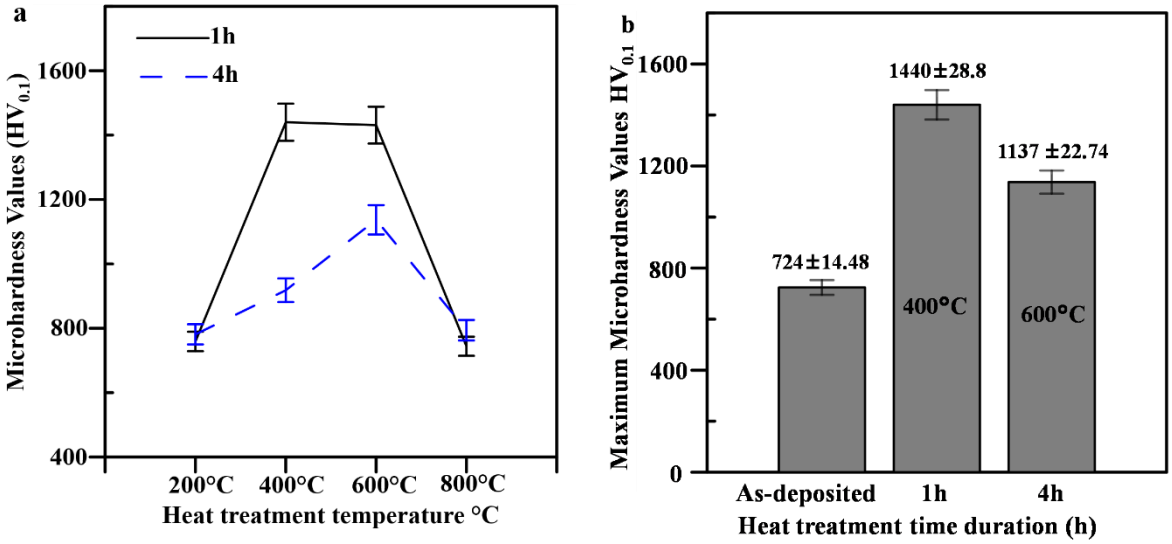

Figure 5. (a) Microhardness plots for the samples; **(b)** Maximum hardness value plot.

3.4. Friction performance.

EN coatings are uniform and smooth and normally display a low cof. For the present coatings, the cof values are quite low, as presented in Figure 6. It is interesting to see that cof of the coating decreases after heat treatment due to the rise in microhardness of the deposit. The harder coating leads to a lower contact area, resulting in low cof. However, the lowest cof is displayed by coatings undergoing heat treatment at 200°C, 1h, which doesn't yield the best microhardness. The cof reduction is almost 50% (w.r.t. as-deposited coating) as seen in Fig. 6b. In case of 400°C, 1h, reduction in cof is almost 40%. The highest cof is observed for the heat treatment cycle of 600°C, 1h, which is quite hard but also has oxide patches. The cof again decreases for sample heat treated at 800°C, 1h, which may be because of the formation of the higher oxide film, which presents lower shear strength, thus reflecting as low cof. For 4h heat treatment cycles, the cof values are marginally lower for 600°C and 800°C. This may be due to the formation of a higher amount of oxidation which presents a layer of low shear strength. Overall, cof is found to be more or less consistent for samples particularly heat treated at 400°C. The cof values over the testing period are also found to be quite consistent (refer to Figure 7). These plots exhibit an initial period of increasing cof, post which the cof attains almost a stable value. This initial period is known as the run-in period and is a characteristic feature of any wear test in sliding mode.

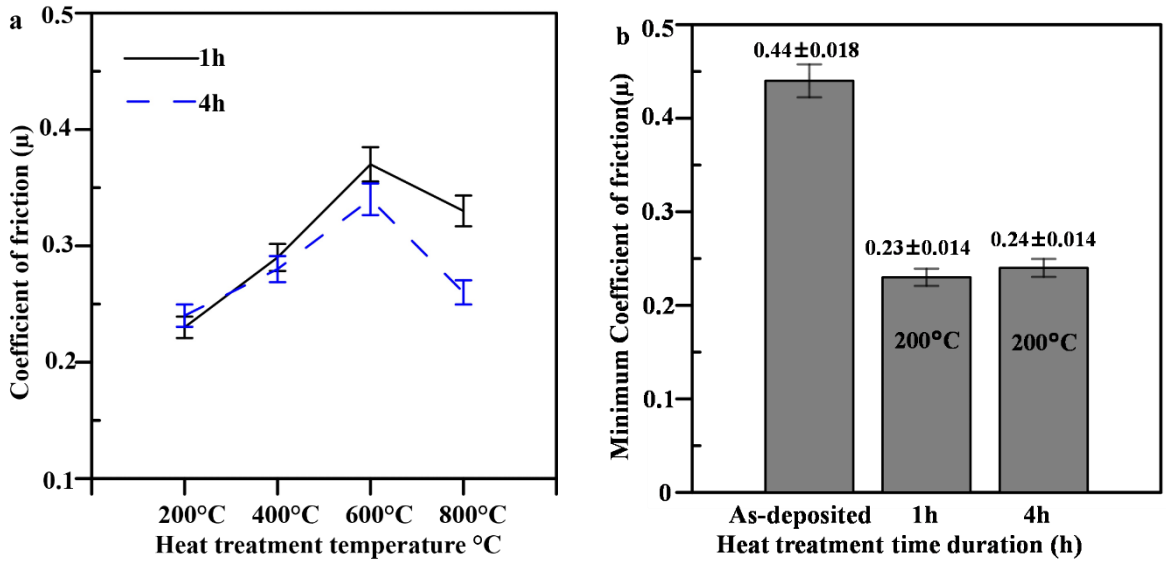

Figure 6. (a) Co-efficient of friction plots and **(b)** Minimum coefficient of friction plot.

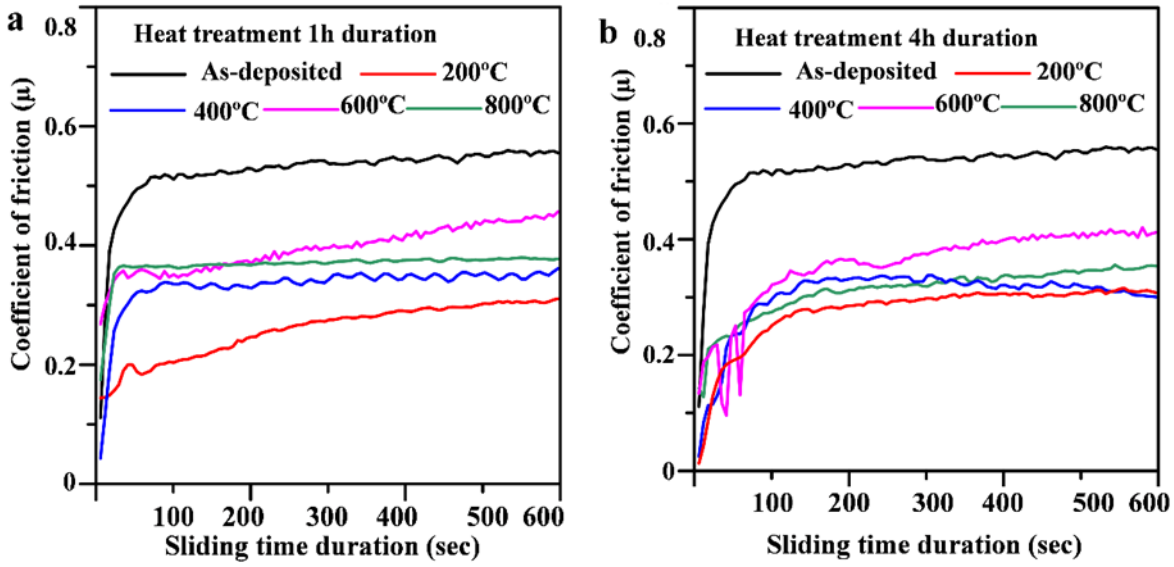

Figure 7. Plot for cof vs. sliding duration **(a)** 1h and **(b)** 4h heat treatment cycle.

3.5. Wear behavior.

The results of the wear test are shown in Figure 8. The top Ni-W-P layer is hard and quite wear-resistant compared to the binary Ni-P coatings. This is because when introduced in the Ni-P matrix, tungsten results in solid solution strengthening. It is observed that the wear rate of the present duplex coatings decreases after heat treatment for 1h duration. In fact, the best wear resistance, as anticipated, is seen for the sample heat-treated at 400°C, 1h (about 50% decrease in the wear rate compared to the as-deposited sample). After heat treatment, harder nickel phosphide phases precipitate (as observed in diffraction results), which increases the microhardness of the coating.

Moreover, upon heat treatment at 400°C, the coating system attains complete crystallization resulting in optimum grain size as well as the correct amount of Ni_3P precipitation. With heat treatment temperature beyond 400°C, the wear rate increases, which may be due to a combination of phenomena, viz. grain coarsening, oxide formation, and interdiffusion of elements. A longer heat treatment period also doesn't seem to have a positive

effect on the wear performance of the coating. However, a good correlation between the wear and microhardness results can be observed for the present coatings, especially for the 1hr heat treatment cycle. The coating displaying the highest hardness displays the lowest wear rate. And as the hardness decreases with higher treatment temperature and longer duration, the wear rate also increases.

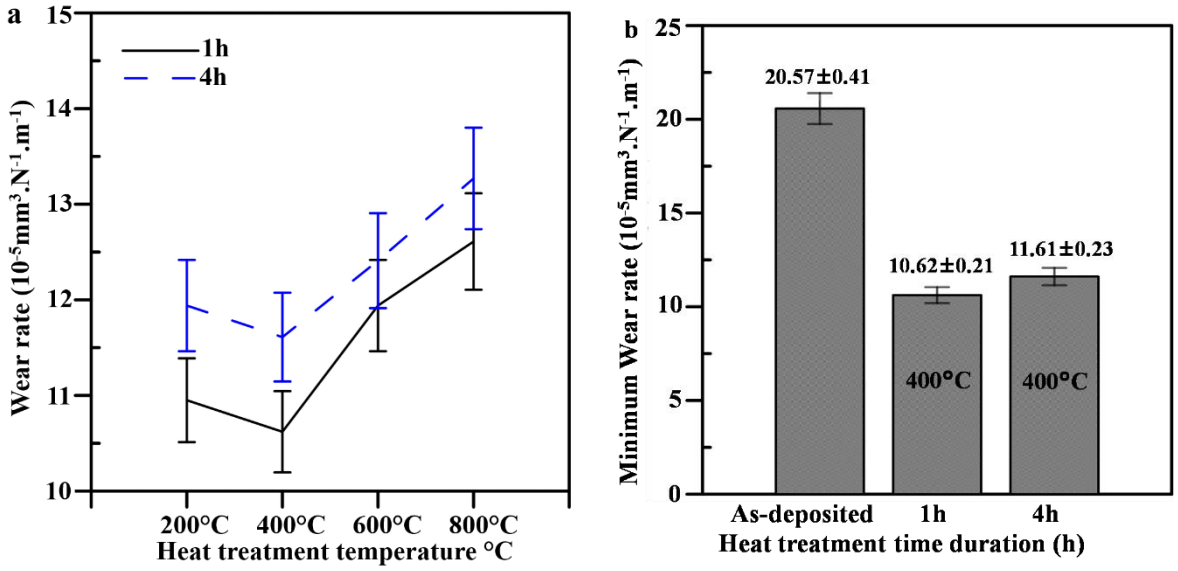

Figure 8. (a) Wear rate for heat-treated coatings and **(b)** Plots for minimum wear rate.

3.6. Wear mechanism.

To study the wear mechanism, the SEM micrograph of a couple of tested samples is given in Figure 9. The 400°C for 1h heat-treated sample (refer to Figure 9a) shows the presence of wear tracks, indicating that an abrasive wear mechanism exists. Some remnants of the original nodular structure of the coating are visible. Apart from the wear tracks, some debris is found to be scattered on the tested surface (marked by arrows). This debris seems to get welded to the surface. A few pits and prows are observed on the worn surface. These imply the occurrence of asheive wear alongside. The wear debris naturally gets pressed between the sample and the counter face, and three body abrasion also seems to be quite probable.

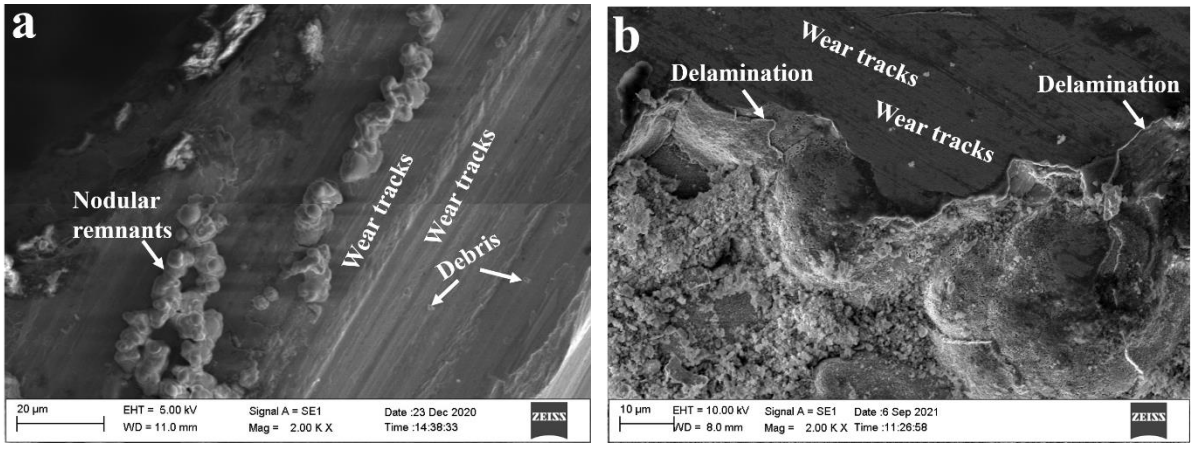

Figure 9. SEM of the sample after wear test **(a)** Heat treated at 400°C for 1h, **(b)** Heat treated at 800°C for 4h.

However, the worn surface of 800°C for 4h heat-treated sample shows a lot of damage (refer to Figure 9b). Apart from wear tracks, a part of the coating layer seems to have

delaminated, exposing the interlayer of the coating. This strongly points out the heavy oxidation suffered by the sample during heat treatment, as already discussed before. Now, the top oxide layer doesn't have the necessary adhesive strength with the coating interlayer making it vulnerable to flaking and delamination under contact pressure. Wear debris in patches is also found to be smeared on the worn surface of the sample. The SEM micrograph of the sample is quite commensurate with its higher wear rate, as observed during the wear test.

3.7. Corrosion.

The results of PDP and EIS tests for the present duplex Ni-P/Ni-W-P coatings are listed in Table 2. The PDP plots of the present Ni-P/Ni-W-P duplex coatings are presented in (Figure 10). The plots exhibit proper Tafel region with distinct anodic and cathodic sections. The PDP results show that, in general, the corrosion potential moves towards the positive region after heat treatment. This implies that as-deposited coatings have the least corrosion resistance. This is interesting, considering present as-deposited coating is believed to possess an amorphous structure.

In fact, heat treatment induces crystallinity in the coating that may aid corrosive media in penetrating the coating by traveling through the grain boundaries. Hence, the present observation may be explained by the fact that the present coating has more of a nanocrystalline structure rather than completely amorphous. After heat treatment, the coating becomes denser and more compact. This type of observation has been reported by some other researchers as well [22]. Besides, as the present coating is a duplex coating system, heat treatment may help attain a splendid adhesion between the two layers of deposit.

Another interesting thing to observe is that the corrosion potential moves towards the positive direction with higher heat treatment temperature, especially for a 1h heat treatment cycle (Figure 10a). This may be because of the fact that with higher heat treatment temperatures, grain coarsening of the coating occurs. Now, coarser grains are always favorable w.r.t. resisting the corrosive media.

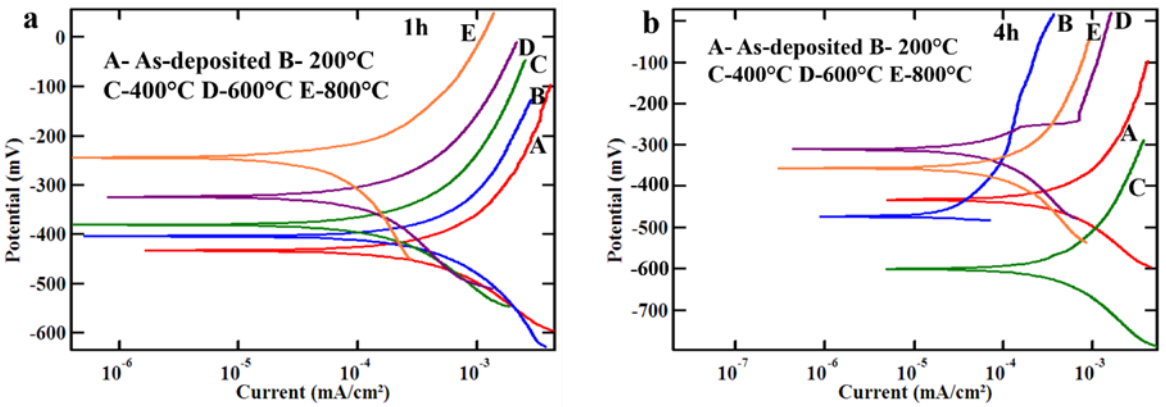

Figure 10. PDP plot of the coatings **(a)**1h and **(b)** 4h duration.

In the case of the 4h heat treatment cycle, the samples display higher corrosion resistance than as-deposited coatings except for the sample heat-treated at 400°C, 4h. The Nyquist plots for the present coating are shown in Figures 11a and 11b, while the equivalent circuit employed is illustrated in Figure 11c. The EIS plots for the samples processed with a 1h heat treatment cycle display one semicircle. The semicircle is specifically located in the high-frequency region at OCP of the respective coatings (refer to Figure 11a).

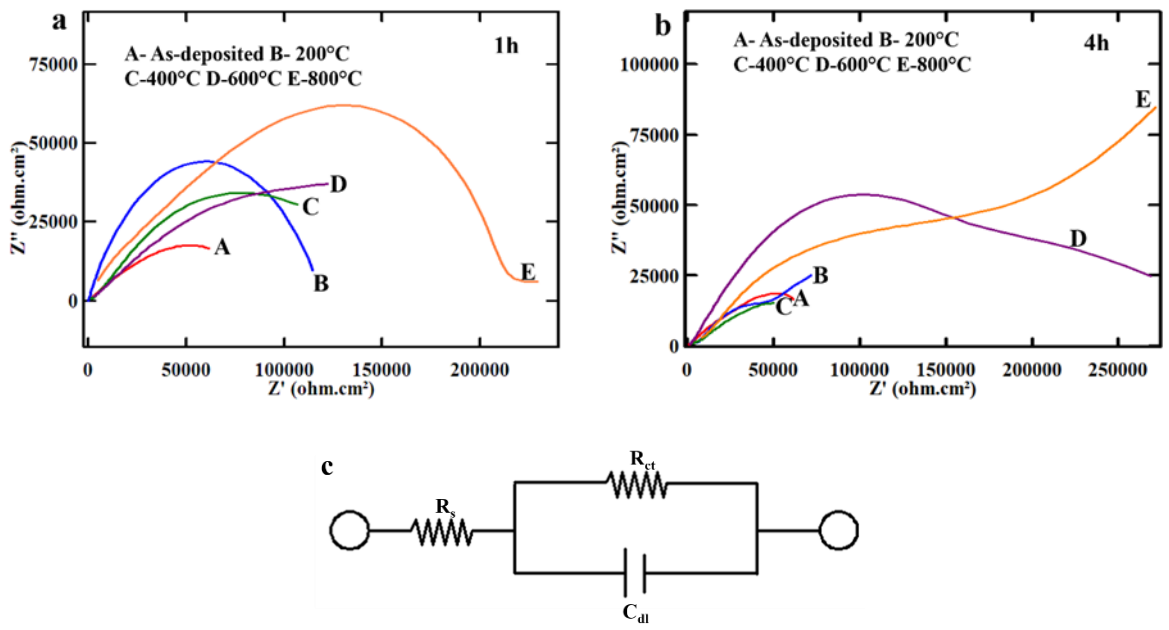

Figure 11. Nyquist plots of the coatings **(a)** 1h duration, **(b)** 4h duration, and **(c)** equivalent circuit diagram.

Table 2. Corrosion data obtained from PDP and EIS tests.

Duplex Ni-P/ Ni-W-P Coating	E_{corr} (mV)	i_{corr} (mA/cm^2)	R_{ct} (ohm.cm^2)	C_{dl} (10^{-4} F)
As-deposited	-433	0.0003488	1.108×105	0.2108
At 200°C 1h	-404	0.0002064	1.407×105	0.0480
At 400°C 1h	-379	0.0001854	1.415×105	0.0984
At 600°C 1h	-324	0.0001470	2.738×105	0.0631
At 800°C 1h	-243	0.0000910	4.030×105	0.0053
At 200°C 4h	-474	0.0003238	2.065×105	0.0546
At 400°C 4h	-602	0.0003218	1.260×105	0.2834
At 600°C 4h	-310	0.0001304	2.247×105	0.0303
At 800°C 4h	-357	0.0000818	2.312×105	0.0148

The existence of a single semicircle in the Nyquist plots specifies that the corrosion process encountered in the present duplex coatings contains a fixed time constant. Moreover, the semicircles are almost similar in shape but vary in size. This implies the same fundamental process must have been encountered during corrosion for all the samples. R_{ct} and C_{dl} values almost reflect the same story as seen in the case of PDP test. Compared to as-deposited coating, heat-treated samples show higher Rct and lower C_{dl} values. The highest R_{ct} value is seen for the sample heat-treated at 800°C, 1h. The results indicate that there may be some minor porosity in the as-deposited coating, which gets reduced after heat treatment. This is supported by the fact the C_{dl} values decrease with an increase in the treatment temperature. The low R_{ct} and high C_{dl} values for the sample heat-treated at 400°C, 4h, is a bit intriguing. Now, during heat treatment, several phases are precipitated in the coating microstructure. This results in inhomogeneities in the material, making it prone to attack by corrosive media. The resulting microstructure may be vulnerable to this attack for the concerned sample, displaying poor corrosion resistance.

In the current study, electroless duplex Ni-P/Ni-W-P coating has been successfully developed with descent microhardness and is found to perform fairly well in friction and wear, and corrosion tests. Post heat treatment, the microhardness of the coating increases in general with enhancement in their performance. However, heat treatment conditions have various

effects on the coating properties. It is observed that the coating achieves the highest hardness at a temperature of about 400°C post, which reduces microhardness due to grain coarsening and oxidation. As a result, the wear resistance suffers when the heat treatment temperature is beyond 400°C. However, there is an improvement in the corrosion resistance ability of the coating. Heat treatment for 4h duration didn't positively impact the coating compared to 1h cycle. Overall, from the investigation, it can be inferred that the optimal heat treatment regime is around 400°C for 1h. Therefore, heat treatment at a higher temperature and duration seems to be superfluous without adding much positive impact on the coating.

Table 3. Comparison of microhardness and wear for binary and duplex coatings

Coating Type	Microhardness ($HV_{0.1}$)		Wear rate (10^{-5} mm3.N^{-1}.m^{-1})	
	AD	HT (400°C,1h)	AD	HT (400°C,1h)
Binary Ni-P	585	1082	25.32	14.52
Binary Ni-W-P	735	1435	18.46	7.53
Duplex Ni-P/Ni-W-P	724	1440	20.57	10.62

*AD-As deposited; HT – Heat treated

Table 4. Comparison of corrosion performance for binary and duplex coatings

Coating Type	E_{corr} (mV)		R_{ct} (ohm.cm^2)	
	AD	HT (400°C,1h)	AD	HT (400°C,1h)
Binary Ni-P	- 386	- 346	1.820×10^5	2.252×10^5
Binary Ni-W-P	- 452	- 403	0.092×10^5	1.125×10^5
Duplex Ni-P/Ni-W-P	- 433	- 379	1.108×10^5	1.415×10^5

*AD-As deposited; HT – Heat treated

The discussion of the present work remains incomplete without a performance comparison between the duplex coatings with the constituent binary coatings. A comparison of the microhardness and wear results is given in Table 3, while the corrosion results are compared in Table 4. It can be observed that the microhardness of the present duplex coating is significantly higher than binary Ni-P coating but marginally lower than binary Ni-W-P coating for both as-deposited as well as heat-treated cases. In fact, Ni-W-P as the top layer also increases the wear resistance of Ni-P coatings, further enhancing through heat treatment. This is quite logical, considering tungsten in the Ni-P matrix induces a solid solution-strengthening mechanism, as already discussed before.

Interestingly in the case of corrosion performance, however, the present duplex coatings perform inferiorly relative to binary Ni-P coatings with lower E_{corr} and R_{ct} values. Now, the corrosion behavior in the Ni-P system is affected by the P content as the same decides the formation of passive film on the coating surface, thus protecting it. Hence, the binary Ni-P coating used for the comparison study is developed with approximately the same P percentage as the present duplex coatings. However, the duplex coatings performed fairly well compared to binary Ni-W-P coatings. Thus, it can be seen that the duplex coatings combine the advantages of the individual constituent layers, thus being able to provide a decent combination of wear and corrosion resistance. This makes them ideal material candidates for demanding applications.

To date, EN coatings have majorly been applied in their binary [23-25] and ternary forms [26-30]. Recent studies on the incorporation of composite particles viz. Al_2O_3 [31], SiC [32], CeO_2 [33], etc., have led to improvements in the mechanical and tribological performances of EN coatings. In fact, keeping in mind the demanding situations faced in industries, the effect of these incorporations on high-temperature tribological performance has

been investigated [31, 34]. EN coatings have also been employed in offering protection to Mg-based nanocomposites [35] as well as Ti-based alloys [36]. However, the application of EN coatings has been limited mostly to a single layer. The development of duplex or multilayer coatings opens the possibility of higher customization and improved performance of the coatings, as indicated in a few recent studies [37]. Hence, the results of the present study are believed to be useful to relevant industries dealing with surface protection and surface engineering-based applications.

4. Conclusions

Duplex electroless Ni-P/Ni-W-P are deposited successfully by sequential deposition. The coating developed has a higher phosphorous level (above 10%). Moreover, the adhesion between the deposited layers is found to be very good. Both heat treatment temperature and duration are found to influence the properties of the coating affecting its performance significantly. The following conclusions can be drawn from the present study.

The microhardness of the coating increases significantly after heat treatment, with the highest microhardness observed for the samples heat treated at 400℃ for 1h.

Beyond 400℃ and for longer heat treatment duration, grain coarsening and oxidation occurs, which negatively impact the microhardness of the coating.

A good correlation between microhardness and wear resistance is observed for the present duplex coatings.

The corrosion resistance of the coating increases post-heat treatment, with higher heat treatment temperatures inducing higher resistance due to the lowering of grain boundaries due to grain coarsening.

Overall, it is found that 400℃ and 1h is the best heat treatment cycle for the present coatings, which enhances their properties resulting in an all-around performance from them.

Funding

This research received no external funding.

Acknowledgments

The first author would like to acknowledge the support received from the Department of Metallurgical & Material Engineering, Jadavpur University, for conducting the XRD experiments.

Conflicts of Interest

The authors declare no conflict of interest.

References

1. Biswas, P.; Das, S.K.; Sahoo, P.; Role of heat treatment on the friction and wear behavior of duplex electroless nickel deposits. *Materials Today: Proceedings*. **2022**, *66*, 3902-3909, https://doi.org/10.1016/j.matpr.2022.06.322.
2. Sahoo, P.; Das, S.K.; Tribology of electroless nickel coatings – a review. *Mater. Des.* **2011**, *32*, 1760–1775, https://doi.org/10.1016/j.matdes.2010.11.013.
3. Engineered Solutions in Surface Finishing: Medical Device Coatings. Available Online: https://advancedplatingtech.com/medical/medical-coatings/ (accessed on 29th August **2022**).

4. Zhang, B.W.; Hu, W. Y.; Zhang, Q.L.; Qu, X.Y.; Properties of electroless Ni−W−P amorphous alloys. *Mater. Charact.* **1996**, *37*, 119−122, https://doi.org/10.1016/S1044-5803(96)00089-7.
5. Wang, L.P.; Gao, Y.; Xu, T.; Xue, Q.J.; A comparative study on the tribological behavior of nanocrystalline nickel and cobalt coatings correlated with grain size and phase structure. *Mater. Chem. Phys.* **2006**, *99*, 96−103, https://doi.org/10.1016/j.matchemphys.2005.10.014.
6. Tsai, Y.Y.; Wu, F.B.; Chen, Y.I.; Peng, P.J.; Duh, J.G.; Tsai, S.Y.; Thermal stability and mechanical properties of Ni−W−P electroless deposits. *Surf. Coat. Technol.* **2001,** 146−147, *9−10*, 502−507, https://doi.org/10.1016/S0257-8972(01)01462-1.
7. Chen, W.Y.; Tien, S.K.; Wu, F. B.; Duh, J.G.; Crystallization behaviors and microhardness of sputtered Ni-P, Ni-P-Cr and Ni-P-W deposits on Tool steel. *Surf. Coat. Technol.* **2004**, *182*, 85-91, https://doi.org/10.1016/S0257-8972(03)00851-X.
8. Vitry, V.; Bonin, L.; Formation and characterization of multilayers borohydride and hypophosphite reduced electroless nickel deposits. *Electrochim. Acta.* **2017**, *243*, 7–17, https://doi.org/10.1016/j.electacta.2017.04.152.
9. Chen, X.M.' Li, G. Y.; Lian, J.S.; Deposition of electroless Ni−P/Ni−W−P duplex coatings on AZ91D magnesium alloy. *Trans. Nonferrous Met. Soc. China.* **2008**, *18*, 323−328, https://doi.org/10.1016/S1003-6326(10)60225-7.
10. Sankara Narayanana, T.S.N.; Baskaranb, I.; Krishnaveni, K.; Parthibanc, S.; Deposition of electroless Ni−P graded coatings and evaluation of their corrosion resistance. *Surf. Coat. Technol.* **2006**, *200*, 3438−3445, https://doi.org/10.1016/j.surfcoat.2004.10.014.
11. Biswas, A.; Das, S.K.; Sahoo, P.; Correlating tribological performance with phase transformation behavior for electroless Ni-(high) P coating. *Surf. Coat. Technol.* **2017**, *328*, 102-114, https://doi.org/10.1016/j.surfcoat.2017.08.043.
12. Kundu, S.; Das, S.K.; Sahoo, P.; Friction and Wear Behavior of Electroless Ni-P-W Coating Exposed to Elevated Temperature. *Surf. Interfaces.* **2019**, *14*, 192-207, https://doi.org/10.1016/j.surfin.2018.12.007.
13. Sankara Narayanan, T.S.N.; Krishnaveni, K.; Seshadri, S.K.; Electroless Ni-P/Ni-B duplex coatings: Preparation and evaluation of microhardness, wear and corrosion resistance. *Mater. Chem. Phys.* **2003**, *82*, 771-779, https://doi.org/10.1016/S0254-0584(03)00390-0.
14. Keong, K.G.; Sha, W.; Malinov, S.; Hardness evolution of electroless nickel-phosphorus deposits with thermal processing. *Surf. Coat. Technol.* **2003,** *168*, 263–274, https://doi.org/10.1016/S0257-8972(03)00209-3.
15. Palaniappa, M.; Seshadri, S.K.; Structural and phase transformation behaviour of electroless Ni– P and Ni–W–P deposits. *Mater. Sci. Eng. C.* **2007**, *460–461*, 638–644, https://doi.org/10.1016/j.msea.2007.01.134.
16. Lewis, D. B.; Marshall, G.W.; Investigation into the structure of electrodeposited nickel-phosphorus alloy deposits. *Surf. Coat. Technol.* **1996**, *78*, 150–156, https://doi.org/10.1016/0257-8972(94)02402-2.
17. Sahoo, P.; Wear Behavior of Electroless Ni-P Coatings and Optimization of Process Parameters Using Taguchi Method. *Mater. Des.* **2009**, *30*, 1341–1349, https://doi.org/10.1016/j.matdes.2008.06.031.
18. Mohanty, D.P.; Barman, T.K.; Sahoo, P.; Characterisation and corrosion study of electroless Nickel-Boron coating reinforced with alumina nanoparticles. *Mater. Today: Proc.* **2019**, *19 Part 2*, 317-321, https://doi.org/10.1016/j.matpr.2019.07.216.
19. Manning, P.E.; The Effect of Scan Rate on Pitting Potentials of High-Performance Alloys in Acidic Chloride Solution. *Corrosion* **1980**, *36*, 468-474, https://doi.org/10.5006/0010-9312-36.9.468.
20. Biswas, A.; Das, S. K.; Sahoo, P.; Investigation of the tribological behavior of electroless Ni-W-P coating pre and post phase transformation regime. *Mater. Res. Express.* **2019**, *6*, 0965c1, https://doi.org/10.1088/2053-1591/ab33bd.
21. Zhao, Y.; Zhang, J.; Microstrain and grain-size analysis from diffraction peak width and graphical derivation of high-pressure thermomechanics. *J. Appl. Crystallogr.* **2008**, *41*, 1095–108, https://doi.org/10.1107/S0021889808031762.
22. Rabizadeh, T.; Allahkaram, S.R.; Zarebidaki, A.; An investigation on effects of heat treatment on corrosion properties of Ni–P electroless nano-coatings. *Mater. Des.* **2010,** *31*, 3174-3179, https://doi.org/10.1016/j.matdes.2010.02.027.
23. Barman, M.; Barman, T.K.; Sahoo, P.; Effect of Coating Bath Parameters on Properties of Electroless Nickel-Boron Alloy Coatings. *IJSEIMS.* **2022**, *10*, 26, https://doi.org/10.4018/IJSEIMS.2022010101

24. Das, S.K.; Sahoo, P.; Electroless Nickel-Phosphorus Deposits. In Electroless Nickel Plating: Fundamentals to Applications, 1st ed.; Delaunois, F.; Vitry, V.; Bonin, L., Eds.; Taylor & Francis CRC Press, Boca Raton, USA; **2019**, *56*, 446, https://doi.org/10.1201/9780429466274.
25. Barman, M.; Barman, T.K.; Sahoo, P. Effect of borohydride concentration on tribological and mechanical behavior of electroless Ni-B coatings. *Mater. Res. Express.* **2019**, *6*, 126575, https://doi.org/10.1088/2053-1591/ab58b7.
26. Biswas, A.; Das, S.K.; Sahoo, P.; Oxidation issues during heat treatment and effect on the tribo-mechanical performance of electroless Ni-P–Cu deposits. *Proc. Inst. Mech. Eng. L.* **2021**, *235*, 1665-1685, https://doi.org/10.1177%2F1464420721999823.
27. Biswas, A.; Das, S.K.; Sahoo, P.; Effect of copper incorporation on phase transformation behavior of electroless nickel- phosphorous coating and its effect on tribological behavior. *Proc. Inst. Mech. Eng. L.* **2020**, *235*, 898-916, https://doi.org/10.1177%2F1464420720981602.
28. Kundu, S.; Das, S.K.; Sahoo, P.; Tribological behavior of autocatalytic Ni–P–B coatings at elevated temperatures. *Appl. Phys. A.* **2019**, *125*, 1-20, https://doi.org/10.1007/s00339-019-2816-1.
29. Mukhopadhyay, A.; Barman, T.K.; Sahoo, P.; Co-deposition of W and Mo in electroless Ni–B coating and its effect on the surface morphology, structure, and tribological behavior. *Proc. Inst. Mech. Eng. L.* **2020**, *235*, 149-161, https://doi.org/10.1177%2F1464420720956270.
30. Biswas, P.; Samanta, S.; Dixit, A.R.; Sahoo, R.R.; Investigation of mechanical and tribological properties of electroless Ni-P-B ternary coatings on steel. *Surf. Topogr.* **2021**, *9*, 035011, https://doi.org/10.1088/2051-672X/ac11c9.
31. Kundu, S.; Das, S.K.; Sahoo, P.; Influence of Alumina Particles on Tribology of Autocatalytic Ni-P Coatings at High Temperature. *IJSEIMS*. **2021**, *9*, 25, https://doi.org/10.4018/IJSEIMS.2021010101.
32. Vaibhav, N.; Chatterjee, S.; Evaluation of microstructural, mechanical, and tribological characteristics of Ni-B-W-SiC electroless composite coatings involving multi-pass scratch test. *Mater. Charact.* **2021**, *180*, 111414,. https://doi.org/10.1016/j.matchar.2021.111414.
33. Deniz, G.; Erhan, D.; Hatem, A.; Improved wear behaviors of lead-free electroless Ni[sbnd]B and Ni-B/CeO2 composite coatings. *Surf. Coat. Technol.*, **2021**, *422*, 127525, https://doi.org/10.1016/j.surfcoat.2021.127525.
34. Mukhopadhyay, A.; Barman, T.K.; Sahoo, P.; High Temperature Tribology of Surface Coatings. In Recent Advances in Layered Materials and Structures, 1st ed.; Sarmila S. Ed.; Springer Nature, Singapore; **2021**, 25-48,. https://doi.org/10.1007/978-981-33-4550-8.
35. Banerjee, S.; Sarkar, P.; Sahoo, P. Improving corrosion resistance of magnesium nanocomposites by using electroless nickel coatings. *Facta Universitatis Series: Mechanical Engineering*. **2021**, *18*, http://casopisi.junis.ni.ac.rs/index.php/FUMechEng/article/view/7833.
36. Cao, J.; Zhao, W.; Wang, X.; Zhao, Y.; Ma, P.; Jiang, W.; Song, G.; The Microstructure and Tribological Behavior of Ultrasonic Electroless Ni-P Plating on TC4 Titanium Alloy with Heat-Treatment. *Ferroelectrics*. **2022**, *589*, 1-11, https://doi.org/10.1080/00150193.2021.1905720.
37. Biswas, P.; Das, S.K.; Sahoo, P.; Deposition of Duplex and Multilayer Electroless Ni–P/Ni–B Coating and Study of Their Wear Resistance. In Advances in Thermal Engineering, Manufacturing, and Production Management, 1st ed., Ghosh, S.K.; Ghosh, K., Das, S.; Dan, P.K., Kundu, A. Eds. *Springer Nature, Singapore* **2021**, 271-278, https://doi.org/10.1007/978-981-16-2347-9_23.